Asian Journal of Chemistry; Vol. 34, No. 8 (2022), 2017-2024

ASIAN JOURNAL OF CHEMISTRY

https://doi.org/10.14233/ajchem.2022.23667

Cellulose Nanofibrils Production from Sugarcane Bagasse: A Comparative Study between Low Energy Selective Oxidation Method and Stone Milling Fibrillation

NGUYEN CHAU GIANG and VU MINH DUC*

School of Chemical Engineering, Hanoi University of Science and Technology, Hanoi, Vietnam

*Corresponding author: Tel: +84 945467576; E-mail: duc.vuminh@hust.edu.vn

Received: 6 December 2021; *Accepted*: 22 March 2022; *Published online*: 18 July 2022; AJC-20881

Sugarcane bagasse (SCB), an abundant agro-industrial residue in Vietnam, was used as a raw material to produce cellulose nanofibrils (CNF). First, SCB pulp was obtained from the raw material of bagasse using a two-fraction method, soda treatment followed by bleaching with Javel solution. Then, the SCB pulp was converted into nano-sized cellulose fibers by subjected to low energy, economical treatment of TEMPO-mediated oxidation. A traditional mechanical method of fibrillation SCB pulp, stone grinding was done for comparison, the produced nanocellulose is referred to as MeSCB. The nanocellulose fibers refer as TOSCB obtained from the TEMPO oxidation process were characterized in terms of carboxyl content, morphology, crystallinity and thermal stability. The degree of fibrillation and the dimension of the two obtained nanocelluloses was determined by applying FE-SEM observations combined with an image processing application, ImageJ. The results show that the MeSCB were much less nanofibrillated than the corresponding TOSCB material but less toxic.

Keywords: Nanocellulose, Stone grinding, Sugarcane bagasse, TEMPO-oxidation.

INTRODUCTION

Among the cellulose sources, lignocellulosic biomass is the most attractive for the production of nanocellulose. The properties of the plant-based nanocelluloses are dependent on the properties of the fibers in the lignocellulosic biomass, the cellulose isolation process and the method employed for nanocellulose production. The initial stage in the manufacture of nanocelluloses from biomass is to generate a cellulose-rich pulp by treatments to remove lignin and hemicellulose completely or partially, followed by a bleaching process [1].

Cellulose nanofibrils are the long particles of cellulose elementary fibrils with a diameter in the range of server to a hundred nanometer that have both crystalline and non-crystalline regions. The disintegration of the cellulose fibers to obtain cellulose nanofibril can be achieved by mechanical methods, such as homogenization or microfluidization at high pressure [2], nanogrinding [3] and ultrasonication [4] or by chemical methods like acid hydrolysis [5,6], enzymatic hydrolysis and oxidation method [7]. Although mechanical isolation is more environmentally favourable since less chemicals are required, the technique is usually coupled with the considerable energy usage [8].

In recent years, oxidation methods to prepare cellulose nanofibrils from different plant sources have been reported by several researchers as a low energy consuming method. Saito *et al*. [9] extracted cellulose nanocrystals from 2,2,6,6- tetramethylpiperidinyl-1-oxy radical (TEMPO) oxidized wood celluloses combined with moderate mechanical disintegration. Wang *et al*. [10] isolated cellulose nanocrystals from bleached sugarcane bagasse pulp by ultrasonic-assisted TEMPO-mediated oxidation and one-step ammonium persulfate oxidation methods with fixed oxidizer content. Cellulose nanofibrils was created for 3D-printing from sugarcane bagasse by Chinga-Carrasco *et al*. [11]. Alkaline cooking and a combination of hydrothermal treatment and alkaline cooking were used to process bagasse. Before homogenization, the resultant pulps were subjected to two levels of TEMPO-mediated oxidation [11]. Isogai *et al.* [12] showed that TEMPO oxidation with a high NaClO concentration (> 10 mmol/g) followed by 10-20 min of tip sonication could be employed to generate cellulose nanocrystals from pinus and cotton fibers. Similarly, Rezende *et al.* [13] reported the TEMPO-mediated oxidation under an excess of oxidant agent (25 and 50 mmol/g of NaClO) was applied to organosolv pulping and bleached pulp cellulose

extracted from sugarcane bagasse. The TEMPO-oxidized cellulose pulp was further applied ultrasonication to complete nanofibrillation.

Sugarcane bagasse (SCB) is an abundant fibrous waste and agro-industrial waste produced in the sugar extraction process in tropical areas. Every year, mills in Vietnam squeeze 15 million tons of sugarcane to produce 4.5 million tons of bagasse [14,15]. For the large-scale production of nanocellulose fibers, SCB is considered an appealing feedstock because of the concentration, low recalcitrant and abundance of low-cost raw materials. Furthermore, the sugarcane's thin-walled vessel structures play a crucial role in fibre breakdown and cellulose nanofibrils separation [1]. Considerable research has been conducted on the isolation of nanocellulose from sugarcane bagasse ranging from mechanical disintegration [6,16,17] to chemical methods [13,17,18]. However, the influence of varied NaClO oxidant concentrations on carboxyl content, as well as the relationship between the degree of oxidation and nanofibrillation yield, mechanical properties of the cellulose nanofibrils, has rarely been thoroughly studied.

This work aimed to study the suitability of biomass residues from sugarcane bagasse (SCB) as a new source for the lignocellulosic nanofiber production on large scale by a low energy consumption method. Therefore, this study explored the extraction of cellulose pulp from crude SCB using alkaline treatment combined with bleaching using familiar chemicals in daily life such as Javel water. The obtained pulp was characterized in terms of chemical composition and physical properties and used for the production of CNF by exclusive step treatment of TEMPO-mediated oxidation. The influence of NaClO oxidant concentrations on the degree of TEMPO oxidation, which affects the yield of cellulose nanofibril formation and its mechanical properties, was discussed.

EXPERIMENTAL

Sugarcane bagasse (SCB) was collected from extracted sugarcane juice vendors throughout the city of Hanoi ,Vietnam and then boiled in water to remove residual sugar and water-soluble components. TEMPO was supplied by Sigma Aldrich. Sodium hypochlorite solution (*ca.* 12% active chlorine) was supplied by Guangzhou Chemical Reagent Factory. All other chemicals were analytically pure (Guangzhou Chemical Reagent Factory) and used without prior purification.

Preparation of SCB pulp: The dried SCB was digested at 90 ºC in a 3% NaOH solution for 4 h. This eliminated most of the lignin and much of the hemicellulose that generated long fibers of dark yellow SCB. Due to the persistent discoloration, the products were bleached later with bleached water/distilled water = 15/95 v/v by immersing SCB fiber in 6 h at pH = 3-4 maintained by acetic acid (consistent of 3%) to remove any residual lignin and hemicellulose that may have been present. The SCB pulp obtained from the bleaching process has been washed repeatedly with distilled water to reach a neutral pH and used as starting material for the production of nanocellulose.

TEMPO-mediated oxidation of SCB pulp: TEMPO-oxidized SCB nanocellulose (TOSCB) was prepared using the following procedure: SCB pulp (5 g oven-dry pulp) was suspended in deionized water (500mL) containing TEMPO (0.08 g) and NaBr (0.5 g) in a 1000 mL glass beaker. The TEMPO-mediated oxidation of the cellulose slurry was started by adding 12% NaClO solution (3, 6, 9, 12 mmol/g dried SCB pulp). The slurry was continuously stirred using a propeller at room temperature. The pH was maintained at 10-10.5 by adding 0.5 mol/L of NaOH until alkali consumption was no longer observed, indicating that the reaction was completed. Oxidized SCB pulp was identified as TOSCB-3, TOSCB-6, TOSCB-9 and TOSCB-12 based on the NaClO concentration used in the reaction. Then, the products were rinsed abundantly with distilled water by centrifugation at 10000 rpm for some 10 min cycles till neutral using a Sorvall Evolution RC superspeed centrifuge (Thermo Scientific).

Using centrifugation separated the nanofibrillated fraction (contained in the supernatant) from the non-fibrillated and partially fibrillated ones, which retained in the sediment fraction at the same time. The yield of nanofibrillation was then calculated from eqn. 1 [19]:

$$\text{Nanofibrillation yield (\%)} = 1 - \frac{\text{Dry sendiment fraction weight}}{\text{Initial dry SCB pulp weight}} \quad (1)$$

Mechanical fibrillation of SCB pulp: Mechanical SCB nanocellulose (MeSCB) was prepared as follow: Bleached SBC pulp was dispersed in water with a content of 3-4% and passing through the high shear ultrafine friction stone grinder of the MKCA 6-2 equipment (Masuoka Sangyo Co., Japan) up to 20 times.

Characterization: Chemical characterization of raw materials and cellulosic pulps were done in terms of their content in ash, holocellulose, lignin and α-cellulose, according to TAPPI standards T-211, T-222, T-203os61 and T-9m54, respectively.

Carboxyl content of TOSCB: The carboxyl content of the oxidized cellulose C (mmol/g) was determined by the titration method according to ASTM D1926-00, following the NaCl-$NaHCO_3$ method.

Degree of oxidation (DO) per anhydroglucose unit of cellulose was calculated based on eqn. 2:

$$DO = \frac{162C}{1000 - 36C} \quad (2)$$

where C, the carboxyl content (mmol/g), the value of 36 corresponds to the difference between the molecular weight of an anhydroglucose unit and that of the sodium salt of a glucuronic acid moiety

Viscosity of TOSCB dispersion: The rheological properties of TOSCB dispersions were measured at 25 ± 1 ºC by a Brookfield Rotational Viscometer sing an RV1 spindle at 0.5 rpm rotation speeds. Aqueous dispersion (100 mL) at 0.1% consistency were prepared by stirring until a homogeneous system was reached.

FTIR analysis: To determine changes in the chemical structure and functional group during soda cooking treatment, bleaching and oxidation process of the SCB, FTIR was applied on SCB, SCB fiber, SCB pulp and TOSCBs by IRAffinity-1s, Shimadzu (Japan) FT-IR spectrometer. The spectra were collected in a spectral range of 4000-600 cm^{-1}.

X-ray diffraction: XRD analysis was performed on SCB, SCB cellulose fiber, SCB pulp and TOSCB, using a diffractometer D8 ADVANCE X-ray diffractometer (Bruker, Germany) equipped with nickel-filtered Cu*K*α radiation operated at 40 kV and 30 mA. Crystallinity index (CrI) values were calculated according to eqn. 3:

$$\text{CrI}\ (\%) = \frac{I_{200} - I_{AM}}{I_{200}} \times 100 \quad (3)$$

where I_{200} is the intensity value for the crystalline cellulose peak 200 (2θ = 22.6º), while I_{AM} is the intensity minimum between the peaks at 200 and 110 (2θ = 18.7º).

Thermal analysis: Thermogravimetric measurements were performed for dried SCB, SCB fiber, SCB pulp and TOSCB sample to characterize the thermal stability of these samples using a Labsys Evo S60/58988 (France) thermogravimetric analyzer. The samples of approximately 2 mg of each were heated in a Pt crucible from 25 to 600 ºC in air. The heating rate was 10 ºC min^{-1}.

FE-SEM analysis: Microstructures of untreated SCB, SCB fiber, SCB pulp were observed using a Jeol 6360-LV Scanning Electron Microscope. The dimension of two types of nanocellulose fibrils TOSCB and MeSCB were measured using a field emission scanning electron microscope JEOL JSM-7600F operated at 2 kV. The dried nannocellulose were prepared in the form of paper. Measurement of nanofibrills diameter was performed in the FE-SEM images using ImageJ analysis program.

Tensile properties of TOSCB nanopapers: The tensile strength and Young's modulus of the TOSCB nanopapers were tested by a Lloyd testing machine with a cross-head speed of 1 mm/min equipped with a load cell of 500N. The films were prepared by casting method from the 0.2% gel of TOSCBs. The specimens were carefully cut into strips of 50 mm × 5 mm and stuck thin aluminium pieces on both ends before tensile tests. The distance of the nanopaper specimen between aluminium pieces was 30 mm. Ten specimens were tested for an average value. The thicknesses of the nanopapers were about 50 µm.

RESULTS AND DISCUSSION

Extraction of cellulose fibers from SCB: Chemical characterization of the cellulose pulp produced is important, as the presence of non-cellulosic materials in the cellulose-rich pulp can interfere in the subsequent method chosen for nanocellulose production, increasing yield, altering the crystallinity and even generating nanocellulose with potentially new applications. In natural SCB, like all kinds of lignocellulosic biomass, cellulose is embedded in a matrix of lignin and hemicellulose, linked together mainly by covalent bonds [20,21]. Fig. 1 presents the chemical composition of SCB at a different stage of treatment. The SCB, used as raw material for cellulose production, consists of 48.71% of cellulose, 21% of lignin, 26.5% of hemicellulose and ash of 4.7%. This composition of the SCB is similar to that found by Pippo *et al.* [22], but the cellulose content is higher than the mean value of variation between 39.5% and 45.7% given by Rocha *et al.* [23]. After alkaline treatment, the cellulose content was sharply increased

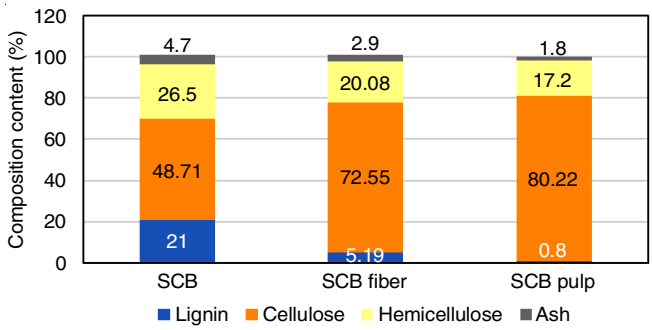

Fig. 1. Effect of treatment condition of the chemical composition of SCB

to 72.55% while the lignin and hemicellulose content was reduced to 5.19% and 20.08%, respectively and the obtained SCB fibres can be observed individually in dark yellow (Fig. 2). The reduction in lignin content suggests that treatment in a 3% NaOH solution could be used as an effective delignification, causing destruction of the links between lignin and cellulose. This removal of lignin has made the cellulose fraction more accessible for further treatment. For further purifying cellulose, bleaching SCB fibers with Javel solution was applied at pH = 3-4, resulting in white SCB pulp (Fig. 2).

From Fig. 1, it is possible to see that the bleaching directly affected cellulose content as a result of removing almost residual lignin and a part of hemicellulose. The bleached SCB pulp was composed of more than 80% of cellulose and 17.2% of hemicelulose while lignin content remained only 0.8%.

Fig. 3 showed the SEM micrographs of the original SCB, SCB fibres and SCB pulp at 100 µm scale, which show the related morphology changes after alkaline treatment and bleaching. The obtained images exhibit substantial differences in the dimension of SCB. The original SCB (Fig. 3a) shows a large bundle of fibrils of some hundred microns in width with a smooth surface while Fig. 3b shows a more disorganized structure and a smaller bundle of alkaline treated SCB fibres. This change could be attributed to the removal of some non-fibrous components in the SCB surface such as lignin, waxes, pectin and oil [6] by NaOH solution at high temperature. Fig. 3c shows that SCB fibres have been separated into individual cellulose fibers of a few microns in diameter. This can be explained by bleaching, which eliminates most of the lignin and hemicellulose of the SCB fibers.

TEMPO-mediated oxidation of SCB pulp and fibrillation of nanocellulose fibers: The TEMPO/NaBr/NaClO oxidation of cellulose pulps at pH 10 and ambient temperature can convert considerable amounts of C6 primary hydroxyl groups to sodium carboxylates. The addition of anionically charged COO- groups to cellulose fibrils in water generates high electrostatic repulsion, allowing for cellulose fiber defibrillation [9]. The higher the degree of oxidation (DO), the more charge is injected and the easier it is for the material to nanofibrillate. To investigate the impact of oxidation conditions on the DO as well as the fibrillation of nanocelluloses from SCB pulp, four levels of NaClO concentration of 3, 6, 9 and 12 mmol/g substrates were being used. The effects of NaClO content on carboxyl content, DO, suspension viscosity and nanofibrilation yield of oxidized SCB pulp are shown in Table-1.

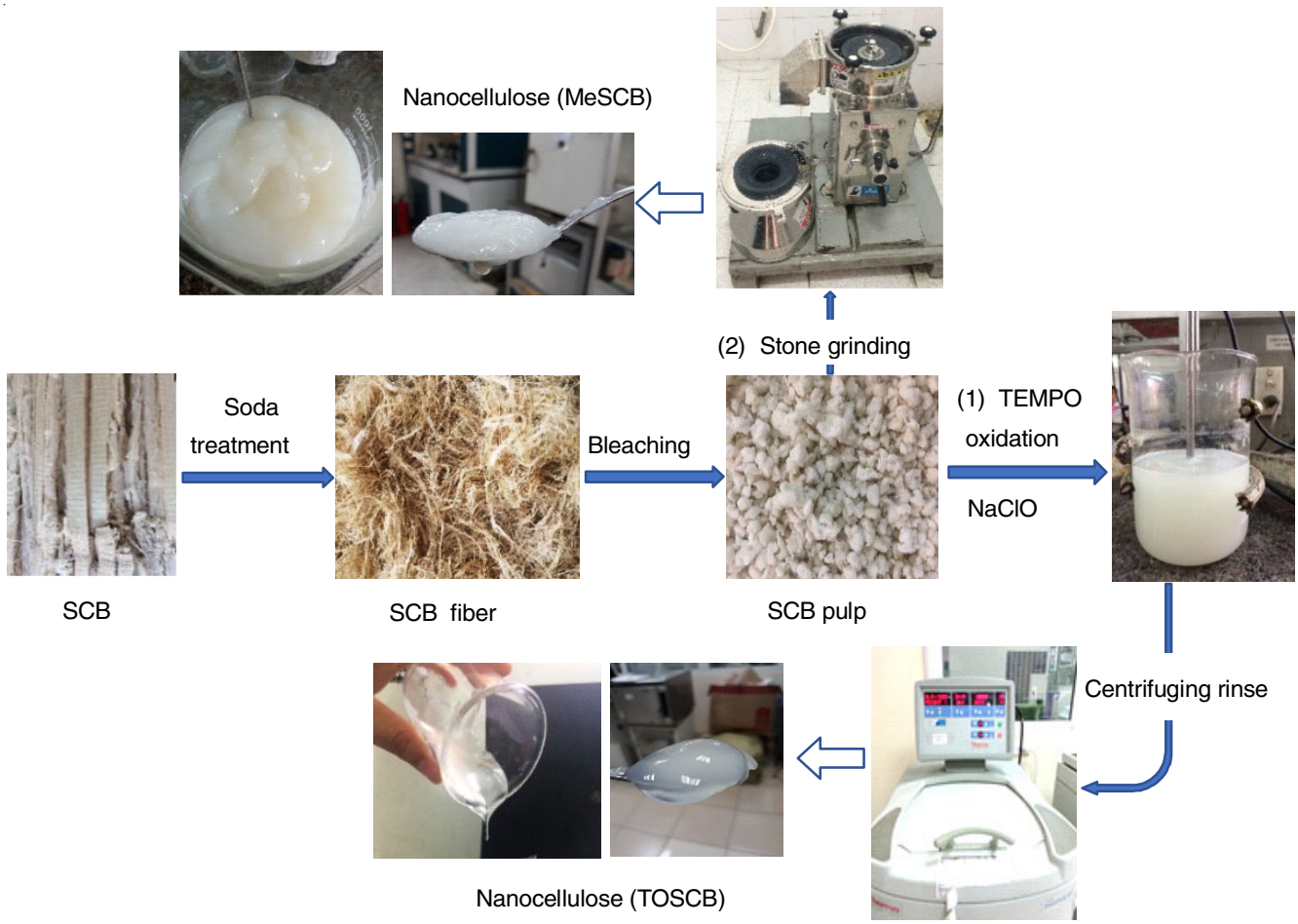

Fig. 2. Procedure of nanocellulose fibrillation from SCB

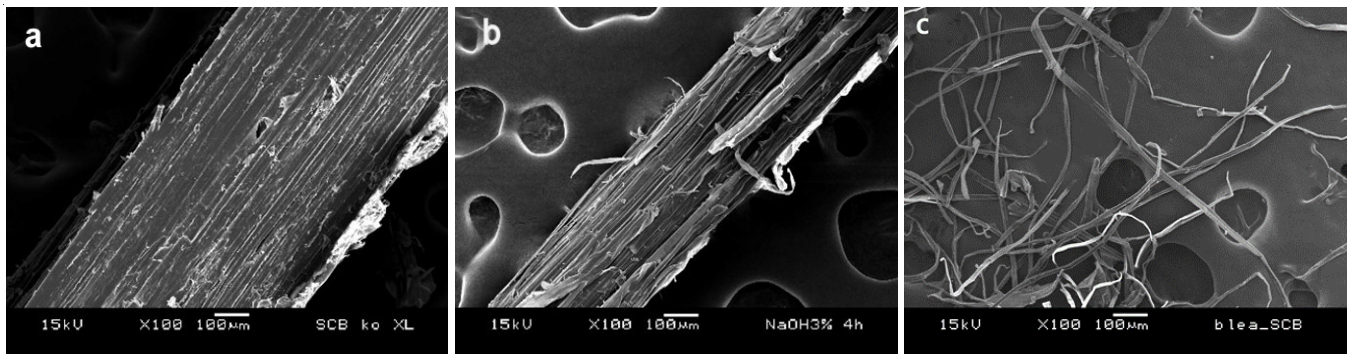

Fig. 3. SEM images of SCB as raw material (a), alkaline treated SCB (b) and bleached SCB pulp (c)

TABLE-1
EFFECT OF OXIDATION LEVEL ON TOSCB CHARACTERISTICS

Sample	C (mmol/g)	DO	Viscosity (Pa.s)	Nanofibrillation yield (%)	Tensile strength (MPa)	Young's modulus (GPa)
SCB pulp	0.002	–	–	–	–	–
TOSCB 3	0.215	0.035	230	50	22.6 ± 8.2	0.90 ± 0.58
TOSCB 6	0.829	0.138	250	74	28.8 ± 10	1.55 ± 0.59
TOSCB 9	1.812	0.314	410	85	30.1 ± 5.1	2.58 ± 0.58
TOSCB 12	1.759	0.304	420	86	31.0 ± 5.0	2.52 ± 0.45

When more NaClO is added during the TEMPO-mediated oxidation, the carboxyl content in oxidized SCB pulp and DO increases, which also increases the cationic demand of the resulting suspension, but increases the NaClO amount beyond 9 mmol did not result in a significant increase in the carboxyl content. At a NaClO concentration of 9 mmol, the degree of

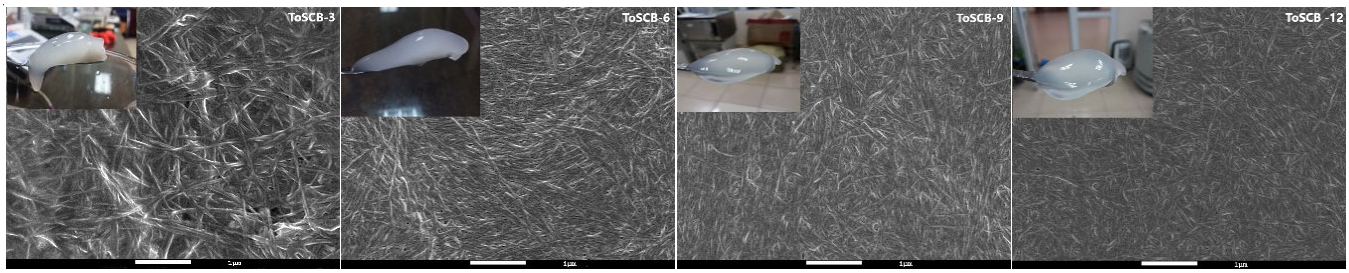

Fig. 4. FESEM pictures of TEMPO-oxidized SCB pulp with different NaClO contents

TEMPO oxidation reached its greatest point of 0.314. Nanofibrillation yield increases as carboxyl content increased, as measured by the amount of nanocellulose fiber recovered after removing the sediment part of nonfibrillated fiber from the bottom of the centrifuge tube. It can be explained by the fact that rise in the carboxyl content has resulted in an increase in the total surface's negative charge, which causes fiber repulsion [9].

The nanofibrillation yield is an indicative measure of the degree of fibrillation of the sample. In other words, an increase in the nanofibrillation yield implies that the cellulose fibers are more nanofibrillated. Transmittance, turbidity and viscosity of the nanofibrils dispersion are also used to determine the degree of fibrillation [24].

As can be seen in Table-1, there was a great difference between the viscosities at 0.1% consistency of four kinds of TOSCB dispersions difference in the carboxylated content. The higher the carboxylated content, the higher the dispersion viscosity and nanofibrillation yield. Furthermore, the higher the carboxylate content, the smaller and more uniform the nanocellulose size becomes, as evidenced by surface FESEM images of TOSCB-9 and TOSCB-12 samples being flatter and smoother than those of TOSCB-3 samples (Fig. 4). With increasing the carboxylate content, the tensile strength of the prepared nanocellulose films increased due to the uniform size distribution.

FTIR analysis: Fig. 5 shows the FTIR spectra of SCB, alkaline SCB fiber, bleached SCB pulp and TEMPO-oxidized cellulose fiber prepared with 12 mmol. It is clear that in all the prepared samples, the FTIR spectra show the absorption bands which are typical of cellu-losic materials, including 3340 cm^{-1} peak for hydrogen-bonded hydroxyl, 2900 cm^{-1} peak for symmetric C-H vibrations and a strong peak at 1041 cm^{-1} for carbonyl group in the backbone structure [10,25]. Fig. 5 also shows that on the alkaline SCB fiber and bleached SBC pulp spectrum, the absorption peak at 1730 cm^{-1}, which is typical for the linkages of esters in lignin and hemicellulose, the peak around 1500 cm^{-1} related to C–H vibration of the aromatic ring in lignin and the peak at 1230 cm^{-1}, which corresponds to C–O stretching in the aryl group of lignin is almost non-existent, which supports after the alkaline treatment, followed by bleaching, effectively removes lignin and hemicellulose. However, in the FTIR spectra of alkaline SCB fiber and bleach SCB pulp, the peak at 1650 cm^{-1}, which corresponds to the aromatic ring found in lignin, can still be seen. This is consistent with the small amount of lignin remaining after alkali treatment

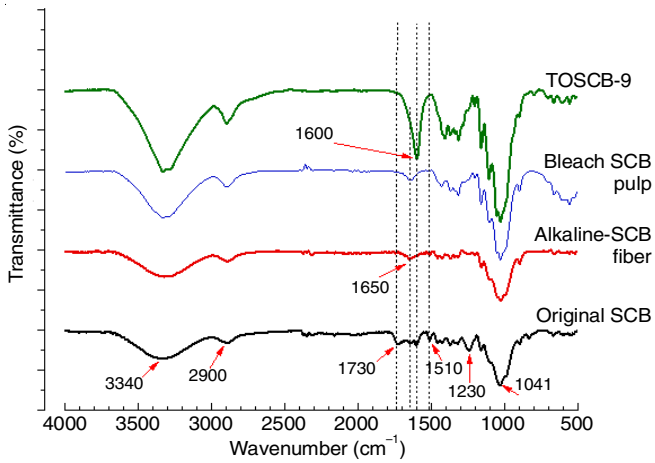

Fig. 5. FTIR spectra of original SCB, alkaline treated SCB cellulose fibers, bleached SCB cellulose pulp and TEMPO oxidation cellulose nanofibers

and bleaching of SCB [27,28]. It is observed that a new peak at 1600 cm^{-1} attributed to C-O stretching frequency of sodium carboxylate were formed in the TEMPO-oxidized bleached SCB pulp, confirming that hydroxyl groups at the C6 position of cellulose molecules were successfully converted to sodium carboxylate [10,28].

XRD studies: Fig. 6 shows X-ray diffraction spectrum of SCB before and after two steps of chemical treatment (alkaline SCB fiber and bleach SCB pulp) and TOSCB-9 nanocellulose fiber. As can be seen from Fig. 6, all the samples showed major diffraction peaks for 2θ at 15.5º and at ranging between 22-23º, corresponding to the (110) and (200) crystallographic planes of the monoclinic cellulose I lattice, respectively [18,29]. Patterns of XRD patterns for all materials were similar indicated that the crystalline morphology of cellulose was preserved during treatment and TEMPO oxidation, however, the crystallinity of the SCB fibers was improved.

The crystallinity indices of each sample determined using the Segal technique revealed that alkaline SCB fiber (69.9%) and bleached SCB pulp (72.8%) have higher crystallinity than the original SCB fiber (63.8%). Due to the biomass composition having a considerable influence on crystallinity [25,30], these changes can be attributed to the removal of amorphous lignin and hemicellulos during chemical treatments. This increase in crystallinity of alkaline treated SCB fiber and bleached SCB pulp compared to original SCB also supports the above SCB composition analysis, as there was an elimination of lignin and hemicellulose caused by alkaline treatment and bleaching

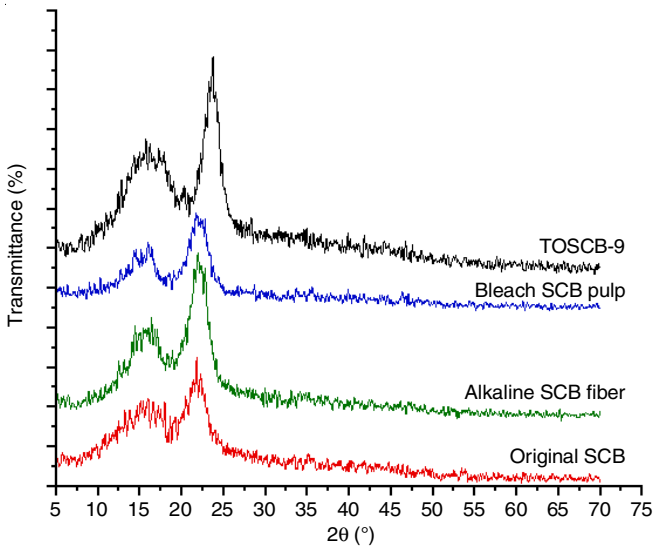

Fig. 6. X-ray diffractograms of sugarcane bagasse, alkaline treated SCB fibers, bleached SCB pulp and TEMPO-oxidized bleached SCB pulp (TOSCB-9)

resulted in an increase in cellulose content. By TEMPO-mediated oxidation, the crystallinity indices of bleached SCB pulp reduced slightly from 72.8% to 71.9%, indicating that part of the crystalline cellulose molecules in the bleached SCB pulp transition to disordered structures with sodium glucuronosyl units. Furthermore, the crystallite size of cellulose in SCB pulp and TOSCB-9 was also calculated from XRD data using the Scherrer's equation [31,32] and found to be 3.371 and 3.376 nm, respectively, demonstrating that no change in the cellulose crystalline structure caused by TEMPO oxidation. Based on the findings that there was only a minor change in the crystallinity index and crystalline size of cellulose in SCB pulp and TOSCB-9 nanofiber, it can be concluded that the TEMPO-mediated oxidation of C6-primary hydroxyls to C6-carboxylates occur mostly on the crystalline microfibril surfaces of this SCB fiber. This result is likewise consistent with the findings of Isogai's investigation [9,32].

Comparison of TEMPO oxidation fibrillation and mechanical refinement nanocellulose: In comparison to the chemical process of TEMPO oxidation, cellulose nanofibrils were made *via* mechanical refining of bleach SCB pulp. The number of passes the fibers made through the grinder had a substantial impact on the level of fiber fibrillation. The bleach SCB pulp fibers depicted in Fig. 3c were lengthy strips with irregular distribution and large size. Due to force shear, some of the long fibers were first chopped into short fibers under mechanical stress and some fibers were flattened during grinding. When the fibers were subjected to grinding for several passes, the majority of the pulp was fibrillated into sub-micron

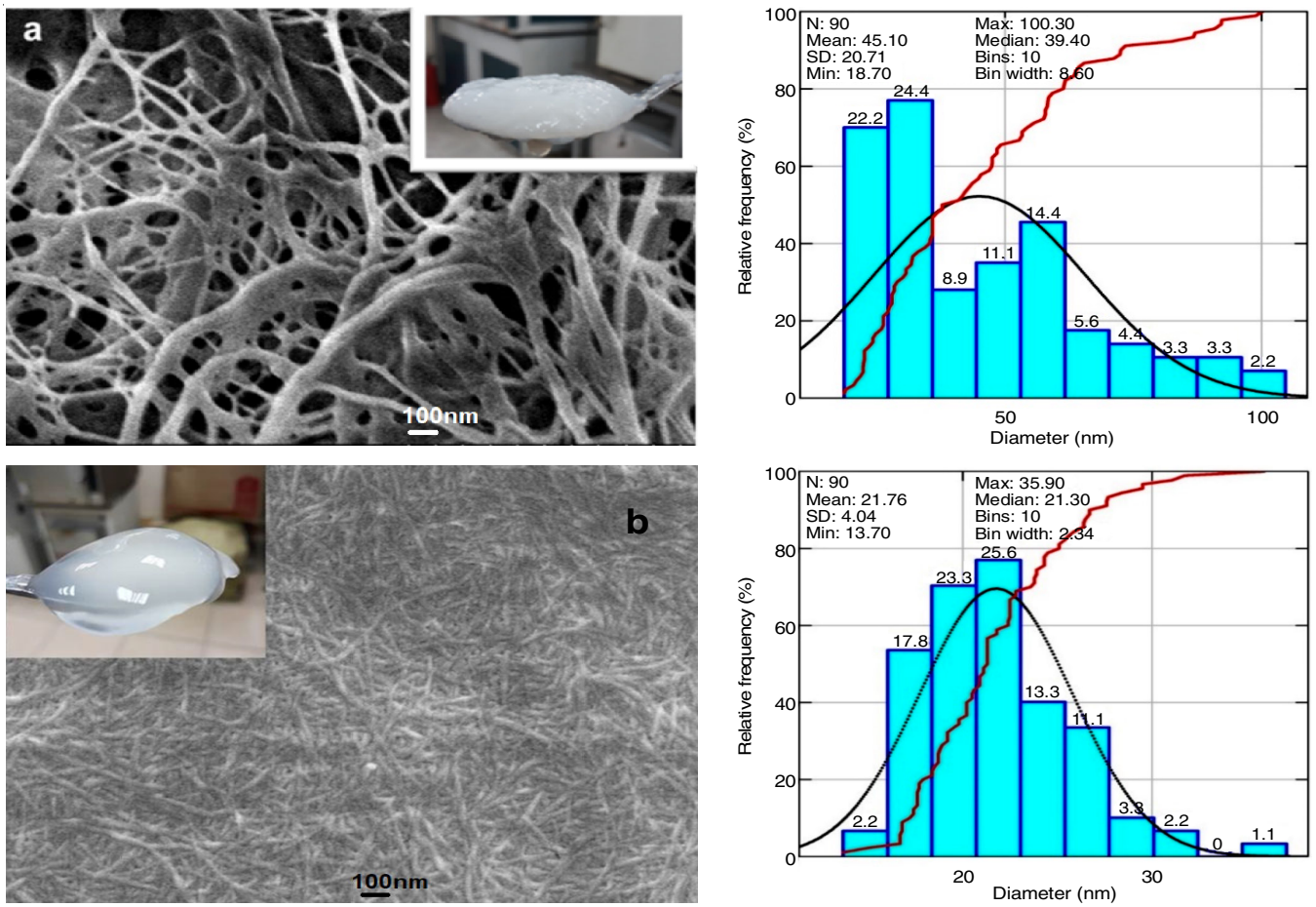

Fig. 7. Comparison of morphology and dimension of cellulose nanofiber extracted from SCB using (a) stone grinder (MeSCB) and (b) TEMPO oxidation (TOSCB)

scale filaments, but a limited number of large size fibers remained. The number of residual fibers significantly decreased as the grinding intensity increased from 10 to 15 passes and the size of the resulting nanofibers became more consistent. After 20 passes through the grinder, the white paste SCB fibers were formed, indicating sufficient fibrillation of the pulp to nanofibers.

Fig. 7 shows the shape of bagasse nanofibers obtained after 20 passes through the grinder and after TEMPO oxidation with a NaClO level of 9 mmol. ImageJ software was used to calculate the size of nanofibers as well as their fiber width distributions and the results are shown in Table-2.

TABLE-2
DIMENSION OF NANOCELLULOSE CALCULATED BASED ON FESEM IMAGES WITH THE SUPPORT OF IMAGE SOFTWARE

Nanofibrils	SCB fiber width range (nm)	Mean dimension (nm)	Standard deviation (nm)
TOSCB	13.7- 35.9	21.76	4.04
MeSCB	18.7- 100.3	45.10	20.71

The foregoing data show that the oxidation approach is substantially more effective in producing nanocellulose from bagasse fibers. To be more specific, the TOSBC fiber produced by the TEMPO oxidation reaction has an average size of 21.76 nm with a small sstandard deviation of 4 nm, whereas the fiber produced by the mechanical approach is more than twice as large, measuring 45.1 nm. Although the mechanical process is simple and does not require the use of chemicals, it produces nanocellulose fibers that are large and irregular in size, as evidenced by the fact that the standard deviation of the fiber diameter is 5 times greater than that of TOSCB. Mechanical grinding, on the other hand, is an extremely energy-intensive process. As a consequence, it can be stated that the TEMPO reaction is able to generate nanomaterial-sized fibers without the use of any additional procedures. Furthermore, because the reaction may be carried out at room temperature, the TEMPO-catalyzed oxidation process is comparatively easy and does not consume as much energy as the mechanical grinding method.

Conclusion

In conclusion, two types of cellulose nanofibers were produced from crude sugarcane bagasse using TEMPO-mediated oxidation and colloid grinder techniques. The effects of sodium hypochlorite on carboxyl content, nanofibrillation yield, suspension viscosity and oxidation degree were investigated. The carboxyl content of oxidized cellulose fibers rose as the NaClO content increased, resulting in an increase in nanofibrillation yield, suspension viscosity mechanical properties of the TOSCB film. The TEMPO-mediated oxidation with NaClO (from 9 to 12 mmol/g substrate) produced elementary cellulose fibrils with widths of 21 nm without the addition of a mechanical defibrillation step. Fibrillation was caused by an over abundance of negative charges on the fiber surface caused by oxidation. Mechanical methods that solely rely on the Masuoka colloid grinder are unable to produce dimensionally consistent cellulose nanofibers.

ACKNOWLEDGEMENTS

This research is funded by Hanoi University of Science and Technology (HUST) under grant number T2018-PC-092.

CONFLICT OF INTEREST

The authors declare that there is no conflict of interests regarding the publication of this article.

REFERENCES

1. D. Pradhan, A.K. Jaiswal and S. Jaiswal, *Carbohydr. Polym.*, **285**, 119258 (2022); https://doi.org/10.1016/j.carbpol.2022.119258
2. S.R.D. Petroudy, B. Chabot, E. Loranger, M. Naebe, J. Shojaeiarani, S. Gharehkhani, B. Ahvazi, J. Hu and S. Thomas, *Energies*, **14**, 6792 (2021); https://doi.org/10.3390/en14206792
3. Y. Yang, H. Liu, M. Wu, J. Ma and P. Lu, *Int. J. Biol. Macromol.*, **161**, 627 (2020); https://doi.org/10.1016/j.ijbiomac.2020.06.081
4. N. Shahi, B. Min, B. Sapkota and V.K. Rangari, *Sustainability*, **12**, 6015 (2020); https://doi.org/10.3390/su12156015
5. W.T. Wulandari, A. Rochliadi and I.M. Arcana, *IOP Conf. Ser.: Mater. Sci. Eng*, **107**, 012045 (2016); https://doi.org/10.1088/1757-899X/107/1/012045
6. M.R.K. Sofla, R.J. Brown, T. Tsuzuki and T.J. Rainey, *Adv. Nat. Sci: Nanosci. Nanotechnol.*, **7**, 035004 (2016); https://doi.org/10.1088/2043-6262/7/3/035004
7. M. Jonoobi, R. Oladi, Y. Davoudpour, K. Oksman, A. Dufresne, Y. Hamzeh and R. Davoodi, *Cellulose*, **22**, 935 (2015); https://doi.org/10.1007/s10570-015-0551-0
8. A. Dufresne, *Mater. Today*, **16**, 220 (2013); https://doi.org/10.1016/j.mattod.2013.06.004
9. A. Isogai, T. Saito and H. Fukuzumi, *Nanoscale*, **3**, 71 (2011); https://doi.org/10.1039/C0NR00583E
10. K. Zhang, P. Sun, H. Liu, S. Shang, J. Song and D. Wang, *Carbohydr. Polym.*, **138**, 237 (2016); https://doi.org/10.1016/j.carbpol.2015.11.038
11. G. Chinga-Carrasco, N.V. Ehman, J. Pettersson, M.E. Vallejos, M.W. Brodin, F.E. Felissia, J. Håkansson and M.C. Area, *ACS Sustain. Chem.& Eng.*, **6**, 4068 (2018); https://doi.org/10.1021/acssuschemeng.7b04440
12. Y. Zhou, T. Saito, L. Bergström and A. Isogai, *Biomacromolecules*, **19**, 633 (2018); https://doi.org/10.1021/acs.biomac.7b01730
13. L.O. Pinto, J.S. Bernardes and C.A. Rezende, *Carbohydr. Polym.*, **218**, 145 (2019); https://doi.org/10.1016/j.carbpol.2019.04.070
14. MoiT/GIZ Energy Support Programe, Business Directory on Sugar Industry in Vietnam, Deutsche Gesellschaft für Internationale Zusammenarbeit (GIZ) GmbH (2017).
15. http://sugar-asia.com/vietnams-sugar-mills-await-policies-to-produce-electricity-from-bagasse/.
16. D. Bhattacharya, L.T. Germinario and W.T. Winter, *Carbohydr. Polym.*, **73**, 371 (2008); https://doi.org/10.1016/j.carbpol.2007.12.005
17. J. Tao, Z. Fang, Q. Zhang, W. Bao, M. Zhu, Y. Yao, Y. Wang, J. Dai, A. Zhang, C. Leng, D. Henderson, Z. Wang and L. Hu, *Adv. Electron. Mater.*, **3**, 1600539 (2017); https://doi.org/10.1002/aelm.201600539
18. B. Puangsin, Q. Yang, T. Saito and A. Isogai, *Int. J. Biol. Macromol.*, **59**, 208 (2013); https://doi.org/10.1016/j.ijbiomac.2013.04.016
19. N.V. Ehman, A.F. Lourenço, B.H. McDonagh, M.E. Vallejos, F.E. Felissia, P.J.T. Ferreira, G. Chinga-Carrasco and M.C. Area, *Int. J. Biol. Macromol.*, **143**, 453 (2020); https://doi.org/10.1016/j.ijbiomac.2019.10.165

20. S. Alila, I. Besbes, M.R. Vilar, P. Mutjé and S. Boufi, *Ind. Crops Prod.*, **41**, 250 (2013); https://doi.org/10.1016/j.indcrop.2012.04.028
21. A.K. Chandel, S.S. da Silva, W. Carvalho and O.V. Singh, *J. Chem. Technol. Biotechnol.*, **87**, 11 (2012); https://doi.org/10.1002/jctb.2742
22. W.A. Pippo, C.A. Luengo, L.A.M. Alberteris, P. Garzone and G. Cornacchia, *Waste Biomass Valoriz.*, **2**, 257 (2011); https://doi.org/10.1007/s12649-011-9069-3
23. G.J. de Moraes Rocha, V.M. Nascimento, A.R. Gonçalves, V.F.N. Silva, and C. Martín, *Ind. Crops Prod.*, **64**, 52 (2015); https://doi.org/10.1016/j.indcrop.2014.11.003
24. G. Chinga-Carrasco, *Micron*, **48**, 42 (2013); https://doi.org/10.1016/j.micron.2013.02.005
25. A.A. Guilherme, P.V.F. Dantas, E.S. Santos, F.A.N. Fernandes and G.R. Macedo, *Braz. J. Chem. Eng.*, **32**, 23 (2015); https://doi.org/10.1590/0104-6632.20150321s00003146
26. G.-L. Guo, D.-C. Hsu, W.-H. Chen, W.-H. Chen and W.-S. Hwang, *Enzyme Microb. Technol.*, **45**, 80 (2009); https://doi.org/10.1016/j.enzmictec.2009.05.012
27. S.K. Evans, O.N. Wesley, O. Nathan and M.J. Moloto, *Heliyon*, **5**, e02635 (2019); https://doi.org/10.1016/j.heliyon.2019.e02635
28. P. Lu, Y. Yang, R. Liu, X. Liu, J. Ma, M. Wu and S. Wang, *Carbohydr. Polym.*, **249**, 116831 (2020); https://doi.org/10.1016/j.carbpol.2020.116831
29. X. Sun, Q. Wu, S. Ren and T. Lei, *Cellulose*, **22**, 1123 (2015); https://doi.org/10.1007/s10570-015-0574-6
30. Z. Xu, Q. Wang, Z.H. Jiang, X. Yang and Y. Ji, *Biomass Bioenergy*, **31**, 162 (2007); https://doi.org/10.1016/j.biombioe.2006.06.015
31. A. Patterson, *Phys. Rev.*, **56**, 978 (1939); https://doi.org/10.1103/PhysRev.56.978
32. T. Isogai, T. Saito and A. Isogai, *Cellulose*, **18**, 421 (2011); https://doi.org/10.1007/s10570-010-9484-9